Calculation of the Electron-Phonon Spectral Function of Niobium†

B. N. Harmon

Ames Laboratory-ERDA and Department of Physics
Iowa State University, Ames, Iowa 50011

S. K. Sinha

Solid State Science Division, Argonne National Laboratory, Argonne, Illinois 60439

ABSTRACT

The electron-phonon spectral distribution function, $\alpha^2(\omega)F(\omega)$, has been calculated for niobium. The energy bands and wavefunctions were obtained from a self-consistent APW muffin-tin potential, and the matrix elements were evaluated using the so called rigid ion approximation. The details of the calculation are presented and the results are compared with recent tunneling experiments, which confirm that the electron-phonon interaction is nearly three times larger for transverse phonons compared to the longitudinal phonons. It is shown that screening is of great significance and evidence is given which suggests that the same screening by d-electrons which causes the dips in the phonon dispersion curves of Nb is responsible for enhancing the electron phonon matrix elements and hence T_c. An omission in the formulas of Gaspari and Gyorffy is pointed out.

---

†Work performed for the U.S. Energy Research and Development Administration under Contract No. W-7405-eng-82.

For d- and f-band materials the relationship between normal state and superconducting state properties is still a major problem. In their phenomenological work McMillan[1] and, more recently, Allen and Dynes[2] have shown the importance of and need for a better understanding of such normal state parameters as the electron-phonon interaction, the density of electron states at the Fermi level, and the phonon spectral distribution. These properties are related in a very complicated manner, and sorting out the coupling mechanisms is a formidable task essential for determining the details governing superconductivity in high T_c materials.

We present a first-principles numerical calculation of α^2F for niobium which provides new insight into the electron-phonon interaction. In the first section the details of the calculation are presented and compared with the approach of Gaspari and Gyorffy.[3] The second section gives the results of the calculations and presents a comparison with tunneling experiments made by two different groups[4,5] (The experiments are reported in the proceedings of this conference.).

I. Calculational Considerations

The electron-phonon (e-p) spectral distribution function is given by

$$\alpha^2(\omega)F(\omega) = \frac{1}{N(E_F)} \oint_{E_F} \frac{dS}{|\nabla_k E|} \oint_{E_F} \frac{dS'}{|\nabla_{k'} E|} \sum_j \frac{|\langle \vec{k}|\nabla V \cdot \hat{\epsilon}_j(\vec{k}-\vec{k}')|\vec{k}'\rangle|^2}{2M\,\omega_{\vec{k}-\vec{k}',j}}$$

$$\times\, \delta(\omega - \omega_{\vec{k}-\vec{k}',j}) \qquad (1)$$

where the integrals are over the Fermi surface, $\hat{\epsilon}_j$ and ω_j denote the phonon eigenvectors and frequencies of the jth branch, and $\nabla V \cdot \hat{\epsilon}$ stands for the screened e-p interaction. The e-p mass enhancement given by

$$\lambda = 2\int \alpha^2(\omega)F(\omega)\ \omega^{-1}\ d\omega \tag{2}$$

where $F(\omega)$ is the phonon density of states. It has been customary to approximate this expression by

$$\lambda = \eta / M\langle\omega^2\rangle \tag{3}$$

where

$$\eta = \frac{1}{N(E_F)} \oint_{E_F} \frac{dS}{|\nabla_k E|} \oint_{E_F} \frac{dS'}{|\nabla_{k'} E|} \langle\vec{k}|\vec{\nabla}V|\vec{k}'\rangle \cdot \langle\vec{k}'|\vec{\nabla}V|\vec{k}\rangle \tag{4}$$

and the approximation is made by taking

$$\langle\omega^2\rangle = \int F(\omega)\omega d\omega \ / \ \int F(\omega)\omega^{-1}\ d\omega. \tag{5}$$

A simple method of evaluating η has been devised by Gaspari and Gyorffy[3] (hereafter referred to as G-G). They used the so called "rigid ion" approximation in which ∇V is the gradient of the muffin-tin potential. This procedure ignores the tails of the atomic potentials in the interstitial regions as well as the electronic charge deformation and redistribution associated with the ionic displacements. G-G also

averaged wavefunction coefficients over the Fermi surface, a procedure which John[6] has shown to be valid for cubic monatomic crystals. A drawback of the G-G method is that it precludes the consideration of individual phonons, hence the evaluation of Eq. (1) is not feasible within the G-G framework. A wide application of the G-G method for calculating η has been made by Klein et al.[7]

The calculations presented in this paper used the APW energy bands and wavefunctions of a self-consistent muffin-tin potential.[8] The actual expression used to evaluate the e-p matrix elements is given by Sinha.[9] In testing the computer programs which evaluated Sinha's expression it was discovered that two terms had been overlooked. For completeness we include the correct expression in the Appendix to this paper. It can be shown that if $E_k = E_{k'} = E_F$ then $I_\alpha^{k'k}$ as given in the Appendix is equivalent to the matrix elements assumed by Gaspari and Gyorffy. Thus we are also neglecting screening effects as well as the tails of the atomic potentials in the interstitial region.

There may be some concern as to the appropriateness of a muffin-tin potential for these calculations.[10] Two separate questions naturally arise 1) How good are the wavefunctions and eigenvalues (Fermi surface) obtained from a muffin-tin potential and 2) How good is the electron-phonon matrix element evaluated within this approximation. Fortuitously the first question has been throughly investigated very recently by Naim Elyashar and Dale Koelling who performed a relativistic, self-consistent, $\alpha = 2/3$, APW calculation using a completely general potential.[11,12,13] They found that the energy eigenvalues were surprisingly accurate within

the muffin-tin approximation (e.g. the Fermi energy changed by only 3 mRy in going from a muffin-tin self-consistent potential to a completely general self-consistent potential).[12] The wavefunctions (and therefore the charge density) did show sensitivity to the non-spherical terms in the potential. There was an increased contribution to the L = 4 angular component of the density and non-uniform shifts of the order of 2% to 3% in the angular momentum character of the wavefunctions - generally in the direction of increased anisotropy.[11,12] Although these changes are significant for accurate X-ray analysis or for understanding the anisotropy in accurate induced form factor measurements by neutron diffraction, the changes are not as important for our calculations. In fact the greatest significance to us of the Elyashar and Koelling results is to give confidence in the wavefunctions we are using from the muffin-tin potential. Of particular concern (as emphasized in the G-G technique) is the ℓ-character of the wavefunctions at the Fermi surface. A comparison between the α = 2/3 muffin-tin and general self-consistent potential results indicated that there were less than 2% differences in the different ℓ components of the density of states at the Fermi level.[13,14]

The problem of assessing the quality of muffin-tin e-p matrix elements has not received as much attention. By only considering the contribution to the matrix element inside the muffin-tin spheres we are neglecting the contribution in the interstitial region. This is probably not too serious an approximation for the following reasons: 1) 85% of the d electron density is contained within the muffin-tin sphere for d-states at the Fermi energy, and p-d and d-f coupling is by far the dominant

contribution to η; 2) the potential in the interstitial region is slowly varying. In future work we intend to investigate the size of the interstitial contribution, however we believe the more serious approximation which deserves immediate attention is the neglect of screening for these matrix elements. A procedure for including screening is outlined in our other paper in these proceedings, and further details will be published elsewhere.

The integrations over the Fermi surface were accomplished by adopting the clever tetrahedron methods which have been developed for evaluating the density of states.[15,16] The irreducible 1/48th of the Brillouin zone is divided into many small tetrahedrans. Inside each tetrahedron the energy bands are linearly interpolated between the four corner energies. As the number of small tetrahedrons increases the linear approximation converges to the correct analytic result. Within a tetrahedron a constant energy surface is a plane whose area can easily be obtained, as can the gradient, $\nabla_k E$. In our calculations the Fermi surface cut through 231 tetrahedrons in the 1/48th of the Brillouin zone. Wavefunctions were evaluated at the center of mass of each of the 231 planes compromising the 1/48th section of the Fermi surface. The summation over $\vec{k}'$ in Eq. (1) requires $\vec{k}'$ to vary over the entire Fermi surface so that group theory is required to rotate those wavefunctions obtained in the 1/48th into the other sections of the complete zone. Our procedure then was to pick a $\vec{k}$ in the 1/48th for which the incremental area ΔS and the gradient were known and let $\vec{k}'$ vary over the other 231 x 48 independent wavefunctions. In this manner $\alpha^2(\omega)F(\omega)$ or $\lambda_{\vec{k}}$ can be obtained for each $\vec{k}$. In principle we should have summed over all 231 $\vec{k}$ in the 1/48th,

but because of computational expense the summation was truncated. The 73 $\vec{k}$ which had the largest weight ($\Delta S/|\nabla_k E|$) were included. These account for 67% of the total density of states at the Fermi energy, and result in 816, 651 total matrix elements. Because each $\lambda_{\vec{k}}$ was calculated the convergence could be watched and we believe our final results are accurate to within 3%. This is supported by the comparison with the calculation of η by the G-G method as described below. The phonon frequencies and eigenvectors were obtained for each of the 816,651 matrix elements using an 8th nearest neighbor force constant fit.[17]

While evaluating $\alpha^2 F$ we also calculated η as given in Eq. (4). Expanding the wavefunctions in the angular momentum representation inside the muffin-tin spheres the s-p, p-d, and d-f contributions to η have been evaluated and are given in the first row of Table I. The row labeled G-G(1) gives results using the G-G method as published.[3,6] The discrepancy between the results was traced to the neglect by G-G of a term arising from the discontinuity in the second derivative of the radial wavefunctions caused by the muffin-tin potential discontinuity at the sphere radius. Understanding how and why this term arises is made clearer by considering appendix 1 in the paper by Evans, Gaspari, and Gyorffy.[18] The radial integral to be evaluated is

$$I = \int_0^{r_s} dr \quad U_\ell \frac{dV}{dr} U_{\ell+1} \tag{6}$$

where in their notation U_ℓ is the radial solution to Schrödinger's equation multiplied by r. Reference 18 shows that the integral is equal

to

$$I = \left[\tfrac{1}{2}(U''_{\ell+1}\, U_\ell + U''_\ell\, U_{\ell+1}) - U'_{\ell+1}\, U'_\ell + \frac{(\ell+1)}{r}\,(U'_{\ell+1}\, U_\ell - U'_\ell\, U_{\ell+1})\right]_{r=0}^{r=r_s} \tag{7}$$

To evaluate this expression the value of the radial wavefunction and its derivatives at the sphere radius are required. Evans, Gaspari, and Gyorffy substitute the values of the radial wavefunction and its derivatives that are valid just outside the muffin-tin sphere - which is equivalent to keeping the unphysical singularity at the muffin-tin sphere in Eq. (6). An appropriate form of the radial function in the interstitial region where the potential is zero is

$$\frac{U_\ell}{r} = R_\ell(r) = j_\ell(\sqrt{E}\, r)\ \cos\,\delta_\ell(E) - n_\ell(\sqrt{E}\, r)\ \sin\,\delta_\ell(E) \tag{8}$$

where $\delta_\ell(E)$ are the scattering phase shifts of the muffin-tin potential evaluated at the sphere radius. With the normalization of Eq. (8) and using atomic units Eq. (7) yields

$$I = \sin(\delta_\ell - \delta_{\ell+1}) + V(r_s) U_\ell\, U_{\ell+1} \tag{9}$$

where $V(r_s)$ is the value of the muffin-tin potential just inside the muffin-tin sphere. The integral in Eq. (6) can easily be evaluated numerically and shows that Eq. (9) is indeed correct. The second term in Eq. (9) has been neglected previously. The row labeled G-G(2) are the results using the corrected formula. The small remaining differences are

probably due to the lack of convergence in our summations. Our calculation includes cross terms[6] (arising from p-d transitions in one matrix element in Eq. (4) but d-f transitions in the other) and yields a total value of η of 10.33 eV/Å^2.

II. Results

The calculated α^2F function, Eq. (1), is shown as a histogram in Fig. 1 along with the phonon density of states $F(\nu)$. The value of λ obtained from Eq. (2) was 1.87 (equivalent to setting $\langle\omega^2\rangle^{\frac{1}{2}}$ to 183 K). The usual approximation of Eq. (5) yields 195 K for $\langle\omega^2\rangle^{\frac{1}{2}}$ and using Eq. (3) would give λ = 1.64, which shows that the so called "constant α^2" approximation is not very good. The value of 1.87 for λ is about a factor of 2 larger than the range of accepted values[1,2] and strongly suggests that screening effects are important. (We do not expect λ to change greatly with different potential precriptions for calculating the band structure.)

Figure 1 shows that α^2 for the lower transverse peak is enhanced by nearly a factor of three over the α^2 for the longitudinal peak. This is also observed in the tunneling measurements.[19] The tunneling spectra appear to have some broadening probably caused by intrinsic phonon lifetime effects and/or surface effects.[20] Figure 2 shows the tunneling data of Bostock et al.[4,21] from a polycrystalline sample. Although there is some question over the values of μ^* and λ obtained in these experiments

the shape of α^2F seems to be rather insensitive, and we therefore have some justification for comparing the shape of our calculated α^2F with the experimental results.

Surface contamination is a well known problem in tunneling experiments using d-band metals. Some arguments have been made that the high energy phonon induced structure is smeared more than the low energy structure because the high energy electrons have a shorter mean free path and thus are affected proportionately more by the surface crud.[20] In the absence of any rigorous way of taking into account the effect of the surface, we assumed the inverse of the penetration depth to be proportional to the width of a Gaussian function with which we broaden the calculated α^2F histogram of Fig. 1. Results by Lo et al.[21] indicate that this broadening should go as ω^2. We thus broaden with a Gaussian of standard deviation $\sigma = b\omega^2$; where $b = 2.5 \times 10^{-3}$ meV^{-1}, and is adjusted roughly to fit the observed width of the transverse peak. The heights of the two curves have been normalized at the transverse peak as shown in Fig. 2. The agreement at high energy is not very good. Since the energy dependent broadening arguments seemed to be made in order to account for the small longitudinal peak, and since our calculation indicated this is mostly due to α^2; we tried broadening the histogram of Fig. 1 without any energy dependence. The theory curve in Fig. 3 is obtained using a Gaussian of standard deviation .82 meV - which was again picked to give approximately the experimental transverse peak width. Now the high energy region is in substantially better agreement. The preliminary

to give close to the experimental transverse peak width. Now the high energy region is in substantially better agreement. The preliminary results of Robinson, Geballe, and Rowell[22] are shown in Fig. 4. The theory curve in this figure is exactly the same as the theory curve of Fig. 3 except for the change of scale. With the theory curve as a guide the experimental curves of Figs. 3 and 4 are seen to be very similar, with only the low energy region being significantly different. The conclusions given below are qualitative and do not depend significantly on the assumed broadening function.

It is immediately clear that our calculations corroborate the experimental result that the longitudinal phonon peak is suppressed relative to the lower transverse peak, and that this is not an effect caused solely by poor surfaces. In addition the region between the two peaks in the calculated $\alpha^2 F$ is about 30% lower than the observed renormalized spectrum. This indicates screening affects this part of the spectrum less than it does the overall spectrum. In a previous paper[23] we showed that screening by d-electrons near the Fermi level could account for the phonon anomalies observed in many high T_c superconductors (in particular Nb and NbC). A consequence of the ideas developed there was that there should be lessened screening (i.e., relative enhancement) of the e-p interaction in the regions of the anomalies. Specifically the screening of the e-p matrix elements require the elements of the matrix $(\underset{\sim}{1} + \underset{\sim}{V}\underset{\sim}{\chi})^{-1}$ where the elements involve pairs of virtual transitions between pairs of orbital states. $\underset{\sim}{\chi}$ is a generalized susceptibility matrix and $\underset{\sim}{V}$ the q-dependent Coulomb coupling coefficient between charge

density waves corresponding to the transition. For Nb we expect the transitions within the predominantly t_{2g}-like d-band complex at the Fermi surface to dominate. As discussed in Ref. 23 and in our other paper in these proceedings, for a sufficiently high density of states at E_F and a correspondingly large χ, the intra d-band elements of $(\underset{\sim}{1} + \underset{\sim}{V}\underset{\sim}{\chi})$ can become quite small for q near the zone boundary, leading to both anomalies in the dispersion relations and relative enhancement of the e-p matrix elements in those regions. Unfortunately the α^2F spectrum is ω-rather than q- selective, but it is significant that the differences between the two curves in Figs. 3 and 4 correspond exactly to the frequency range of the longitudinal phonons in the regions of the anomalies. In the low frequency region there also appears to be a relative enhancement of α^2F over our calculated spectrum. This may be due to the softening of the low frequency transverse phonons in Nb at low temperatures as observed by Shapiro et al.,[24] compared to the values we used which were based on room temperature data. Experiments are now in progress at the Ames Laboratory research reactor to obtain a more complete analysis of the low temperature phonon dispersion curve of Nb. We should also remark that Shapiro et al. observed stronger coupling to the transverse phonons (about twice as large as the average over all the phonons).

In conclusion, the results of this calculation together with the recent tunneling measurements clearly indicate the importance of screening and suggest that the same d-electron screening effects responsible for the dips in the Nb phonon spectrum also enhance the e-p

interaction and hence T_c as we had speculated earlier.[23] Since this effect is rather sensitive to the density of states at the Fermi level, a corresponding comparison for Mo would be very worthwhile. We have also shown that the rigid ion matrix element calculation yields the correct qualitative features regarding how α^2F differs from F, but that quantitatively it is not a good approximation and neither is the usual practice of separately averaging over the phonons.

The authors wish to acknowledge helpful discussions with D. K. Finnemore, W. Kamitakahara, D. D. Koelling, W. Butler, B. M. Klein, L. Boyer, and D. Papaconstantopoulos. They also wish to thank B. Robinson, T. H. Geballe, and J. M. Rowell as well as J. M. Bostock and M. L. A. MacVicar for sending details of their tunneling data. The authors are grateful to D. Papaconstantopoulos for the Nb self-consistent potential, and M. Mostoller for independently checking the phonon frequency calculations.

REFERENCES

1. W. L. McMillan, Phys. Rev. 167, 331 (1968).
2. P. B. Allen and R. C. Dynes, Phys. Rev. B12, 905 (1975).
3. G. D. Gaspari and B. L. Gyorffy, Phys. Rev. Letters 28, 801 (1972).
4. J. Bostock, V. Diadiuk, W. N. Cheung, K. H. Lo, R. M. Rose, and M. L. A. MacVicar, Phys. Rev. Letters 36, 603 (1976).
5. B. Robinson, T. H. Geballe, and J. M. Rowell, Bull. Amer. Phys. Soc. 21 #3, 402 (1976).
6. W. John, J. Phys. F. 3, L231 (1973).
7. B. M. Klein, D. Papaconstantopoulos, Phys. Rev. Letters 32, 1193 (1974); D. Papaconstantopoulos and B. M. Klein, Phys. Rev. Letters 35, 110 (1975).
8. J. R. Anderson, D. A. Papaconstantopoulos, J. W. McCaffrey, and J. Schirber, Phys. Rev. B7, 5115 (1973). A more accurate determination of $N(E_F)$ per spin gives 9.54 states/Ry-atom rather than the value quoted in this paper.
9. S. K. Sinha, Phys. Rev. 169, 477 (1968).
10. C. Varma in the proceedings of this conference expressed some concern that the muffin-tin approximation was too crude an approximation for his taste.
11. N. Elyashar, Ph.D. thesis, University of Illinois, Chicago (1975) unpublished.
12. N. Elyashar and D. D. Koelling, Phys. Rev. B (in press).
13. N. Elyashar and D. D. Koelling, Phys. Rev. B (to be published).

14. D. D. Koelling (private communication)

15. O. Jepson and O. K. Anderson, Solid State Commun. 9, 1763 (1971).

16. G. Lehman and M. Taut, Phys. Status Solidi B54, 469 (1972).

17. Y. Nakagawa and A. D. B. Woods, Phys. Rev. Letters 11, 271 (1963).

18. R. Evans, G. D. Gaspari, and B. L. Gyorffy, J. Phys. F 3, 39 (1973).

19. References 4, 5, and the proceedings of this conference.

20. L. Y. L. Shen, Superconductivity in d- and f-Band Metals, edited by D. H. Douglass, A.I.P. Conference Proceedings No. 4 (A.I.P., NY 1972).

21. K. K. Lo, J. L. Bostock, M. L. A. MacVicar, and R. M. Rose, M.I.T. Technical Report No. 11, 1975 (unpublished).

22. Reference 5 and the proceedings of this conference.

23. S. K. Sinha and B. N. Harmon, Phys. Rev. Letters 35, 1515 (1975).

24. S. M. Shapiro, G. Shirane, and J. D. Axe, Phys. Rev. B12, 4899 (1975).

Table I

η	s-p	p-d	d-f
Eq. (2)	0.80	4.91	4.18
G.-G. (1)	0.61	3.78	4.53
G.-G. (2)	0.82	4.83	4.11

Comparison of the results of Eq. (4) using 816,651 matrix elements with the results using the method of ref. 3. G.-G. (2) is with the corrected formulas. Units are $eV/\AA^2$.

FIGURE CAPTIONS

Fig. 1. The electron-phonon spectral distribution function, α^2F (histogram), compared with the phonon spectrum $F(\nu)$. Both curves normalized to 3.0.

Fig. 2. The polycrystal tunneling results for α^2F (ref. 4) compared with the energy dependent broadened theoretical α^2F of Fig. 1. The curves are normalized to have the same transverse peak height.

Fig. 3. The same polycrystal tunneling results compared with the broadened theoretical α^2F. The broadening is energy independent and the curves are again normalized at the transverse peak.

Fig. 4. The same theoretical curve as shown in Fig. 3 but compared with the preliminary experimental α^2F of ref. 5.

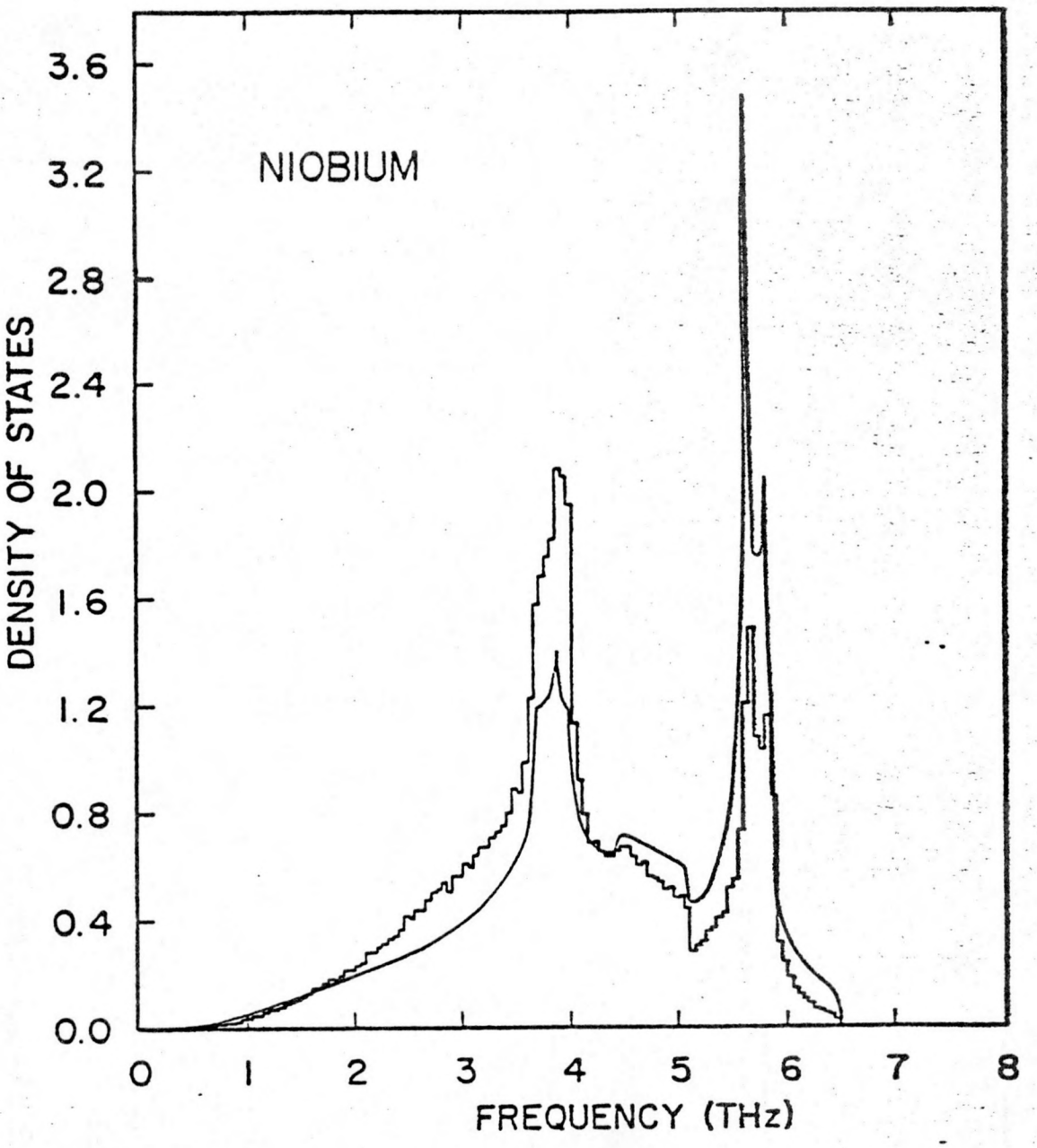

Figure 1. The electron-phonon spectral distribution function, α^2F (histogram), compared with the phonon spectrum $F(\nu)$. Both curves normalized to 3.0.

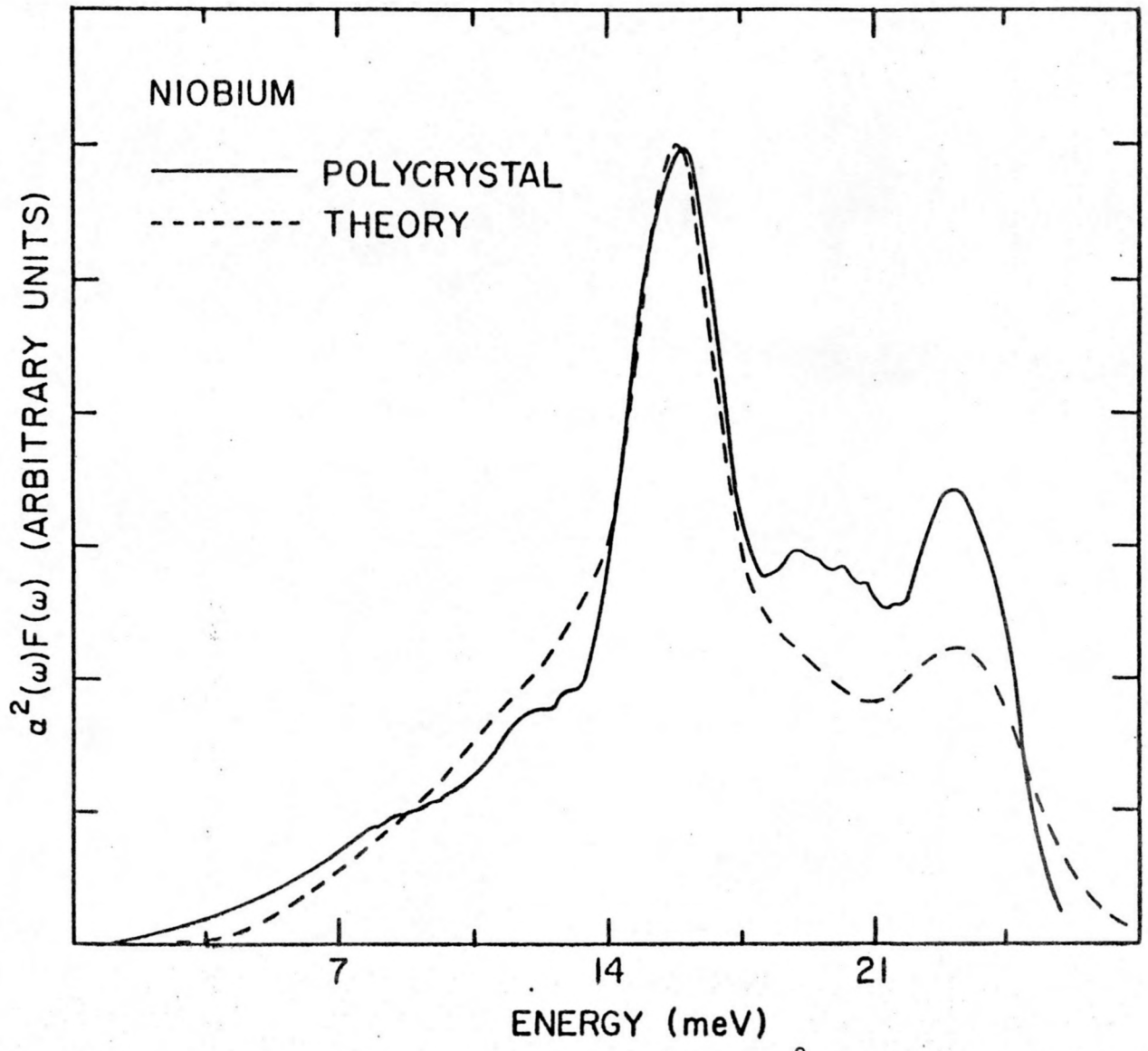

Figure 2. The polycrystal tunneling results for α^2F (ref. 4) compared with the energy dependent broadened theoretical α^2F of Fig. 1. The curves are normalized to have the same transverse peak height.

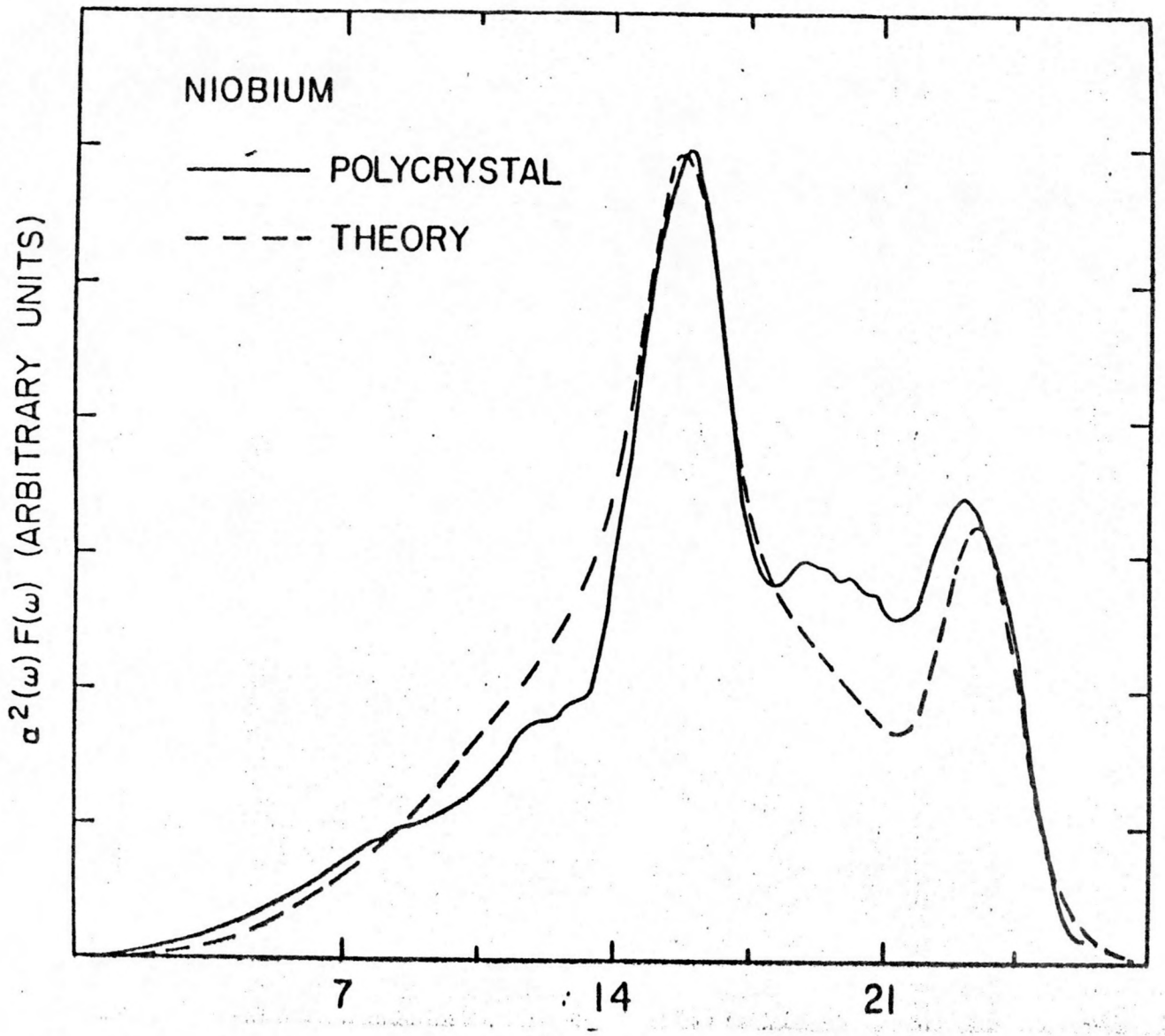

Figure 3. The same polycrystal tunneling results compared with the broadened theoretical α^2F. The broadening is energy independent and the curves are again normalized at the transverse peak.

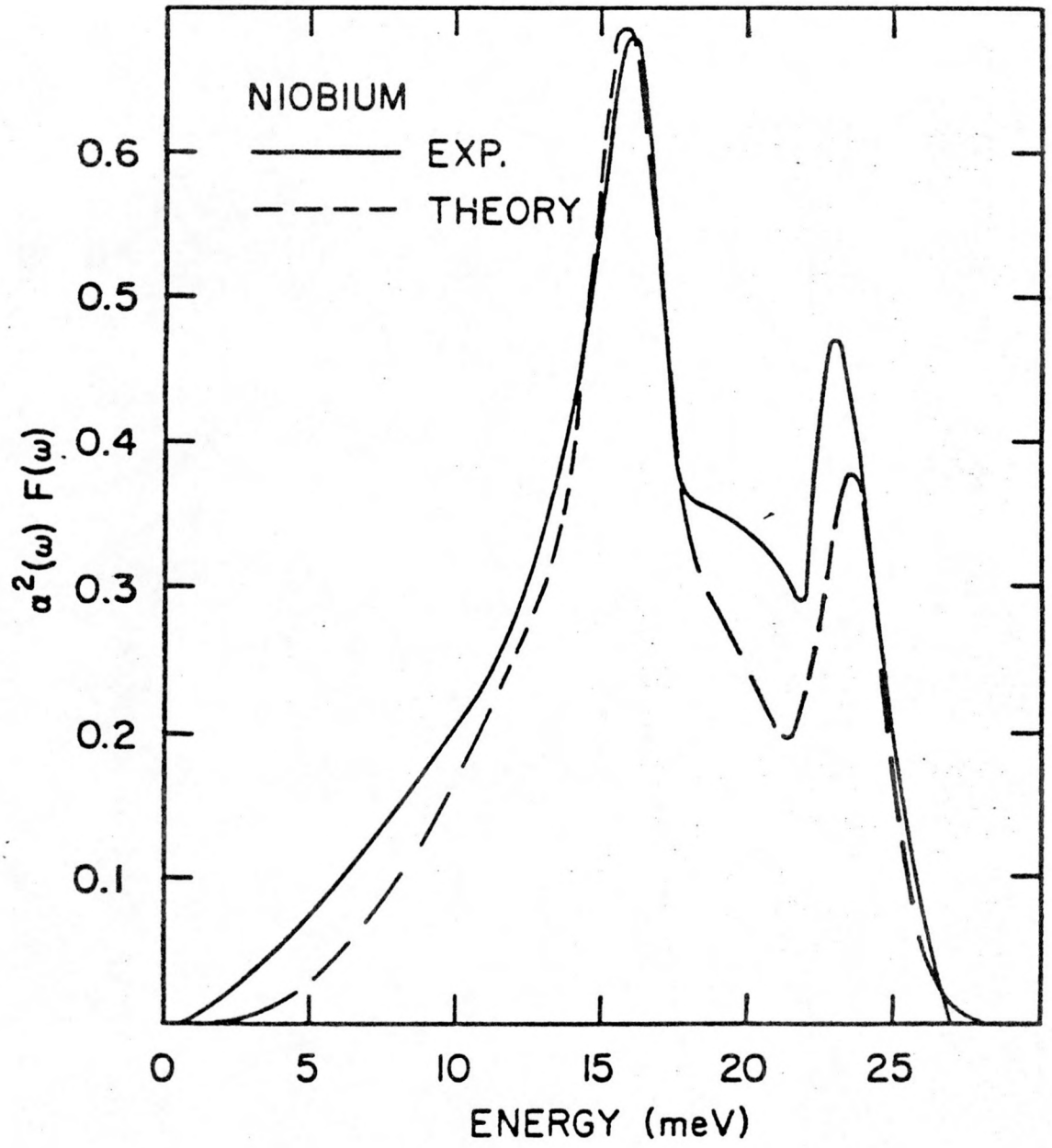

Figure 4. The same theoretical curve as shown in Fig. 3 but compared with the preliminary experimental α^2F of ref. 5.

APPENDIX

A thorough discussion of the electron-phonon matrix element has already been given by Sinha.[9] In this appendix we restrict ourselves to correcting and rewriting the expression [Eq. (A6) of Ref. 9] for the electron-phonon matrix element. The interested reader is referred to Sinha's paper for details concerning notation.

For matrix elements taken within the muffin-tin sphere it is convenient to expand the Bloch functions in the angular momentum representation:

$$\psi_k(\vec{r}) = \sum_{\ell,m} B_{\ell,m}(k)\, R_\ell(r)\, Y_{\ell,m}(\hat{r}) \qquad |\vec{r}| < r_s$$

where r_s is the muffin-tin radius. Then Sinha's Eq. (A6) can be correctly written as

$$I_\alpha^{k'k} = \frac{\hbar^2}{2m}\, r_s^2 \sum_\ell \left\{ \left[\frac{\ell(\ell+2)}{r_s^2} + \frac{2m}{\hbar^2}\,[V(r_s)-E_k] - \left(\frac{2}{r_s} + L_{\ell+1}\right) L_\ell + \frac{\ell}{r_s}(L_{\ell+1}-L_\ell) \right] \right.$$

$$\times (-i) \left(\frac{\ell+1}{2\ell+1}\right)^{\frac{1}{2}} \sum_{m,m'} B_{\ell,m}(k)\, B^*_{\ell+1,m'}(k')\, C^{\ell+1,1,\ell}_{m',m-m'}\, A_{m-m',\alpha}$$

$$+ \left[\frac{(\ell-1)(\ell+1)}{r_s^2} + \frac{2m}{\hbar^2}\,[V(r_s)-E_k] - \left(\frac{2}{r_s} + L_{\ell-1}\right) L_\ell + \frac{\ell+1}{r_s}(L_\ell - L_{\ell-1}) \right]$$

$$\left. \times (i) \left(\frac{\ell}{2\ell+1}\right)^{\frac{1}{2}} \sum_{m,m'} B_{\ell,m}(k)\, B^*_{\ell-1,m'}(k')\, C^{\ell-1,1,\ell}_{m',m-m'}\, A_{m-m',\alpha} \right\}$$

where L_ℓ represents the logarithmic derivative (R'_ℓ/R_ℓ) evaluated at the muffin-tin radius. L_ℓ is evaluated at E_k and $L_{\ell\pm1}$ at $E_{k'}$. For $E_K=E_{k'}$ the epxressions inside the square brackets can be simplified using the scattering phase shifts similar to Eq. (9). In fact if $E_k=E_{k'}=E_F$, and if $I_\alpha^{k'k}$ is used as the matrix elements in Eq. (4) then one obtains exactly the Gaspari-Gyorffy formulation for η (including the correction term discussed with Eq. (9) and the off diagonal term discussed by John[6]).